

RESEARCH PAPER



Up-regulating microRNA-138-5p enhances the protective role of dexmedetomidine on myocardial ischemia-reperfusion injury mice via down-regulating Ltb4r1

Yanzi Chang^a, Lika Xing^a, Wenjuan Zhou^a, and Wei Zhang^b

^aDepartment of Anesthesiology, Attending Doctor, Pain and Perioperative Medicine, The First Affiliated Hospital of Zhengzhou University, Zhengzhou, China; ^bDepartment of Anesthesiology, Chief Physician, Pain and Perioperative Medicine, The First Affiliated Hospital of Zhengzhou University, Zhengzhou, China

ABSTRACT

Both microRNAs (miRs) and dexmedetomidine (Dex) have been verified to exert functional roles in myocardial ischemia-reperfusion injury (MI/RI). Given that, we concretely aim to discuss the effects of Dex and miR-138-5p on ventricular remodeling in mice affected by MI/RI via mediating leukotriene B4 receptor 1 (Ltb4r1). MI/RI mouse model was established by ligating left anterior descending coronary artery. The cardiac function, inflammatory factors and collagen fiber contents were detected after Dex/miR-138-5p/Ltb4r1 treatment. MiR-138-5p and Ltb4r1 expression in myocardial tissues were tested by RT-qPCR and western blot assay. The target relationship between miR-138-5p and Ltb4r1 was verified by online software prediction and luciferase activity assay. MiR-138-5p was down-regulated while Ltb4r1 was up-regulated in myocardial tissues of MI/RI mice. Dex improved cardiac function, alleviated myocardial damage, reduced inflammatory factor contents, collagen fibers, and Ltb4r1 expression while increased miR-138-5p expression in myocardial tissues of mice with MI/RI. Restored miR-138-5p and depleted Ltb4r1 improved cardiac function, abated inflammatory factor contents, myocardial damage, and content of collagen fibers in MI/RI mice. MiR-138-5p directly targeted Ltb4r1. The work evidence that Dex could ameliorate ventricular remodeling of MI/RI mice by up-regulating miR-138-3p and down-regulating Ltb4r1. Thus, Dex and miR-138-3p/Ltb4r1 may serve as potential targets for the ventricular remodeling of MI/RI.

ARTICLE HISTORY

Received 21 May 2020
Revised 12 January 2021
Accepted 15 January 2021

KEYWORDS

Myocardial ischemia-reperfusion injury; dexmedetomidine; microRNA-138-3p; leukotriene B4 receptor 1; ventricular remodeling; myocardial damage

Introduction

Ischemic heart disease remains the prevailing cause of morbidity and mortality around the world [1]. Restoring ischemic myocardial blood flow is one of the most frequent treatment methods for ischemic heart disease, which can minimize the damage induced by the infarct, but sudden recovery of blood flow may lead to extra cardiovascular trauma, that is, reperfusion injury [2]. The molecular mechanism of myocardial ischemic/reperfusion injury (MI/RI) is connected to inflammation, oxidative stress, cytokine release, calcium overload, and infiltration of neutrophil [3]. An epidemiologic study has shown that the risk of I/R injury is connected with gender, age and genetic polymorphism as well as ischemic heart disease [4]. MI/RI may be implicated in the progression of left ventricular remodeling linked to cardiac myocyte death, fibrosis, inflammation, vascular rarefaction, and electrophysiological remodeling, leading to

sudden cardiac death and advancing heart failure [5]. To date, there is a lack of effective therapy for controlling MI/RI and novel therapeutic targets are necessary.

Dexmedetomidine (Dex) has a cardioprotective effect via reducing MI/RI in animal models [6]. It is reported that Dex attenuates renal I/R injury and MI/RI in a dose-dependent manner through suppressing inflammatory response [7]. MicroRNAs (miRs) bind to 3'untranslated region (3'UTR) of the target genes and modulate their expression at the post-transcriptional level [8]. MiRs often refer to the biomarker for pathologies, such as hsa-miR-1307, -miR-3064, -miR-4709, -miR-3615, and -miR-637 in oxidative stress and retinitis pigmentosa [9]. MiR-138-5p exerts suppressive effects on tumors and down-regulated miR-138-5p is closely related to clinicopathological factors and poor survival of patients [10]. A study has presented miR-138 reduces MI/RI by suppressing mitochondria-

mediated apoptosis [11]. Another study has revealed that miR-138 protects cardiomyocytes from hypoxia by regulating glucose metabolism [12]. Leukotriene B4 (LTB4) is a pro-inflammatory lipid mediator derived from arachidonic acid, and binds two G-coupled receptors: the high-affinity LTB4 receptor 1 (BLT1) that is expressed on the surface of immune and inflammatory cells and the low-affinity Ltb receptor 2 (BLT2) [13–15]. A study has presented that suppressing Ltb4r1 signaling pathway through adenosine monophosphate-activated protein kinase activation may be therapeutic for septic cardiac dysfunction in terms of its suppressive effects on cardiac apoptosis, which may occur by the suppression of inflammation and mitochondrial dysfunction [16]. According to Hoog *et al.*, LTB4 concentrations in ischemic myocardial tissues is raised before neutrophil infiltration reaches its maximum [17]. Hence, the effect of Dex on ventricular remodeling in mice affected by MI/RI was evaluated from the perspective of miR-138-5p/Ltb4r1 axis.

Materials and methods

Compliance with ethical standards

All animal experiments were in compliance with the Guide for the Care and Use of Laboratory Animal by International Committees. The protocol was approved by the Institutional Animal Care Use Committee of Pain and Perioperative Medicine, The First Affiliated Hospital of Zhengzhou University.

Experiment animals

One-hundred and thirty-two C57BL/6 J male mice (6–8 w, 5–22 g) were available from Animal Experimental Center of Zhengzhou University (Henan, China). All mice were reared in a single cage in a standard environment with adequate water and food, 12-h light and adequate ventilation.

Establishment of I/R mouse model

Fasted for 12 h with free drinking water, mice were anesthetized with 3% pentobarbital sodium (30–40 mg/kg) and fixed in a supine position. The needle-shaped electrodes of the electrocardiograph

(ECG) were inserted subcutaneously in the limbs of the mice and the standard limb lead-in ECG was recorded. The ventilator was connected after tracheotomy with 2.5 mL tidal volume and 70–80 times/min respiratory rate. The chest was opened between the 3rd and 4th ribs of the left chest wall of the mice. The thoracic cavity was exposed, the pericardium was cut and the heart was exposed. At 2 mm below the inferior edge of the left auricle and the pulmonary conus, a 5–0 nylon was pierced to ligate the left anterior descending coronary artery (LAD) with a small rubber band cannula for 30 min. Gradually darker myocardium, left ventricle cyanosis, poor local movement, and raised ST segment all indicated myocardial ischemia. After 30 min, the blood flow of LAD was restored for 120-min re-perfusion. When the original pale area gradually turned red and the ST segment recovered more than half, it referred to successful reperfusion [18].

Animal treatment

Thirty mice were randomly grouped into 3 groups (n = 10) and underwent sham-operated surgery (open chest without ligating the LAD), I/R modeling as mentioned above, and intravenous injection with Dex (6 µg/kg/h × 10 min + 0.7 µg/kg/h × 15 min before I/R modeling), respectively [19].

Forty mice were distributed into four groups (n = 10) and intramyocardially injected with Ad-Ctr, Ad-miR-138-5p, Ad-Neg and Ad-miR-138-5p-i adenovirus solution (150 µL, 2.0×10^{10} PFU/mL), and subjected to I/R modeling 3 d later [20].

Forty mice were assigned into 4 groups (n = 10) and intramyocardially injected with Ad-Neg, Ad-miR-138-5p-i, Ad-miR-138-5p-i + si-Ltb4r1 NC as well as Ad-miR-138-5p-i + si-Ltb4r1 adenovirus solution (150 µL, 2.0×10^{10} PFU/mL). Three days later, mice were intravenously injected with Dex for I/R modeling.

All adenovirus vectors were purchased from Genechem (Shanghai, China). In brief, pri-miR-138-5p, miR-138-5p RNAi (miR-138-5p RNA interference), or Ltb4r1 siRNA sequences were designed and cloned with GV201 or GV202 and hU6-MCS-CMV-EGFP into the AdMax adenovirus system (Microbix Biosystems, Mississauga, Canada). The

recombinant adenovirus was transfected into HEK293T cells (ATCC, VA, USA) and purified with Adeno-XTM Virus Purification Kit (BD Biosciences; Clontech, Mountain View, CA). The titer of adenovirus was 2.0×10^{10} PFU/mL.

Cardiac ultrasound detection

On the 14th day after operation, the cardiac function indices, left ventricular internal dimension at systole (LVIDs) and left ventricular internal dimension at diastole (LVIDd) were measured by an ultrasonic instrument. Left ventricular ejection fraction (LVEF) and left ventricular shortening fraction (LVFS) were reckoned.

Hemodynamic detection

After cardiac ultrasound detection, mice were connected with a ventilator and their limbs were connected to ECG electrodes. A median incision was made in the neck to expose and isolate the common artery. Administered with heparin intravenously, mice were inserted with a catheter from the right carotid artery to the left ventricle (the other end was connected to a pressure sensor) to observe left ventricular systolic pressure (LVSP), left ventricular end-diastolic pressure (LVEDP) and the maximum rate of rise of left ventricular pressure increase/decrease ($\pm dp/dt_{\max}$).

Collection of myocardial tissue specimens

Mice were euthanized after taking blood from the inferior vena cava. The hearts of mice were extracted and the left ventricular anterior wall in the LAD blood supply area was dissociated. The myocardial tissues were divided into three blocks, one preserved in liquid nitrogen for protein and RNA extraction, one for hematoxylin-eosin (HE) staining and Masson staining, and the last one for Collagen I and Collagen III examination.

Enzyme-linked immunosorbent assay (ELISA)

The kits for interleukin (IL)-6, tumor necrosis factor- α (TNF- α) and IL-1 β (R&D Systems,

Minneapolis, MN, USA) were placed for 30 min. The ELISA plate was added with serum or standard samples of different concentration (100 μ L/well) and incubated for 1 h. The plate was added with biotinylated antibody working solution (100 μ L/well) and incubated for 1 h. Then, 100 μ L enzyme binding solution (without blank control well) was added into each well. The ELISA plate was sealed by a sealing membrane and cultured for 1 h at 37°C (stable temperature and humidity). The plate was added with 100 μ L/well chromogenic agent and reacted for 10–15 min without light exposure, and with 50 μ L stopping solution for reaction termination. The absorbance (A) value was tested by a microplate reader (BioTek, VT, USA). Due to the positive relations between A value and serum IL-6, TNF- α and IL-1 β contents, IL-6, TNF- α , and IL-1 β concentrations could be calculated by drawing standard curve and comparing with A values.

HE staining

Fixed in 4% paraformaldehyde, the tissue block was embedded in paraffin and sectioned. Conventionally processed with dehydration by gradient alcohol, the sections were permeabilized with xylene, stained with hematoxylin and differentiated with 1% hydrochloric acid alcohol. After that, the sections were treated with 1% ammonia water, counter-stained with 1% eosin solution, dehydrated and cleared (75, 90, 95% alcohol, and absolute ethyl alcohol for 5 min, respectively, xylene 10 min \times twice). Finally, the sections were sealed and pictured under a microscope.

Masson staining

Conventionally dehydrated with conventional gradient alcohol, the sections were permeabilized with xylene, dyed with hematoxylin, and treated with water. Followed by that, the sections were immersed into ponceau acid fuchsin, differentiated with 1% molybdophosphoric acid twice (3 min/time) and counter-stained with 1% aniline blue solution. Subsequently, the sections were differentiated with 1% glacial acetic acid solution, cleared

with xylene, and sealed with neutral gum for microscope observation. The semi-quantitative study of myocardial collagen was carried out by image analysis system. Myocardial collagen volume fraction (CVF) was calculated. Five visual fields were randomly selected to calculate the percentage of collagen tissues in each field.

Immunohistochemistry

The tissues sections were fixed for 30 min in 4°C acetone, hatched with the mixture of 30% H₂O₂ and pure methanol (1: 50) to inactivate the endogenous enzyme, blocked with 5% bovine serum albumin and added with primary antibodies Collagen and Collagen III (1: 800, Sigma-Aldrich, SF, CA, USA). The NC was added with PBS instead of the primary antibody. Re-warmed for 45 min at 37°C, the sections were appended with 50 µL secondary antibody for 1 h, added with 50 µL streptavidin–biotin complex solution for 20 min, developed for 15 min with 50 µL diaminobenzidine and observed under a microscope. The reaction was terminated by distilled water. The sections were counter-stained with hematoxylin, soaked in 1% hydrochloric acid alcohol, dehydrated with gradient alcohol, cleared with xylene and sealed with neutral gum. The known positive sections were utilized as the positive control, Collagen and Collagen III were stained to brownish yellow. The optical density values of Collagen and Collagen III were measured.

Reverse transcription quantitative polymerase chain reaction (RT-qPCR)

The total RNA was extracted by miRNeasy Mini kit (Qiagen company, Hilden, Germany) from myocardial tissues. RNA reverse transcription was performed in line with the instructions of TaqMan® MicroRNA reverse transcription kit (ABI Company, Oyster Bay, NY, USA). PCR primers were compounded by Shanghai Sangon Biotechnology Co. Ltd. (Shanghai, China) (Table 1). The obtained complementary DNA was diluted 10 times and performed real-time PCR reaction using TaqMan® MicroRNA Assays

and TaqMan® premix solution. U6 was the internal control of miR-138-5p while glyceraldehyde-3-phosphate dehydrogenase (GAPDH) of Ltb4r1. The data was reckoned by 2^{-ΔΔCt} method.

Western blot assay

Protein was extracted with radio-immunoprecipitation assay cell lysis buffer (Thermo Fisher Scientific, Massachusetts, USA) with the protein concentration detected by protein concentration determination kit (Sigma-Aldrich Chemical Company, St Louis, MO, USA). Separated by sodium dodecyl sulfate polyacrylamide gel electrophoresis, the protein was transferred to a membrane. The membrane was probed with primary antibodies Ltb4r1 (1: 200) and GAPDH (1: 500, Santa Cruz Biotechnology, Inc, Santa Cruz, CA, USA), and re-probed with 4 mL secondary antibody immunoglobulin G/horseradish peroxidase, which was followed by exposure and development. GAPDH was utilized as the internal parameter. The semi-quantitative analysis of protein relative expression was carried out by image analysis software BandScan 5.0.

Dual luciferase reporter gene assay

Jefferson was adopted to predict the target relationship between miR-138-5p and Ltb4r1 and the binding site between miR-138-5p and Ltb4r1 3'UTR. The Ltb4r1 3'UTR fragment was amplified by PCR. The wild type (WT) and the mutant type (MUT) were extracted with the plasmid extraction kit (Invitrogen, Carlsbad, California, USA). The restriction enzyme XbaI and Xho I double endonuclease cleavage was carried out and the product was purified and recovered. The T4 DNA ligase was ligated with luciferase reporter vector pMir-GLO, DH5α competent Escherichia coli was transformed, the plasmid was extracted, identified by XbaI and Xho I and sequenced. The recombinant reporter plasmids of WT and MUT were constructed and named as Ltb4r1-3'UTR-WT and Ltb4r1-3'UTR-MUT. With 5% CO₂ and 37°C, 293 T cells (American Type Culture Collection, VA, USA) were cultured in high glucose

Dulbecco's Modified Eagle Medium (BD Biosciences, San Jose, CA) plus 10% fetal bovine serum and 1% antibiotics, and co-transfected with miR-138-5p mimic/mimic NC and Ltb4r1-3'UTR-WT/Ltb4r1-3'UTR-MUT. The firefly/luciferase activity in cells were detected by luminescence measurements with dual luciferase reporter gene detection kit (Promega Corporation, Madison, WI, USA).

Statistical analysis

All data were interpreted by SPSS 21.0 software (IBM Corp. Armonk, NY, USA). Measurement data were indicated as mean \pm standard deviation. Comparisons between two groups were formulated by *t*-test, and comparison among multiple groups were assessed by one-way analysis of variance (ANOVA) followed by Tukey's post hoc test if data distributed normally. *P* was bilateral test and

P value < 0.05 stood for statistically significant difference.

Results

Dex improves cardiac function and reduces inflammation in MI/RI mice

Cardiac ultrasound detection, hemodynamic detection, and ELISA revealed that (Figure 1(a-e)) mice with MI/RI were presented with impaired cardiac function (reduced LVEF, LVES, LVSP, and \pm dp/dt_{max} values and increased LVIDs, LVIDd, and LVEDP values) and enhanced inflammation (raised IL-6, TNF- α , and IL-1 β contents). Treated with Dex, cardiac function was improved while inflammatory response was suppressed in MI/RI mice. Generally, Dex could improve the cardiac function and reduce the levels of inflammatory factors in MI/RI mice.

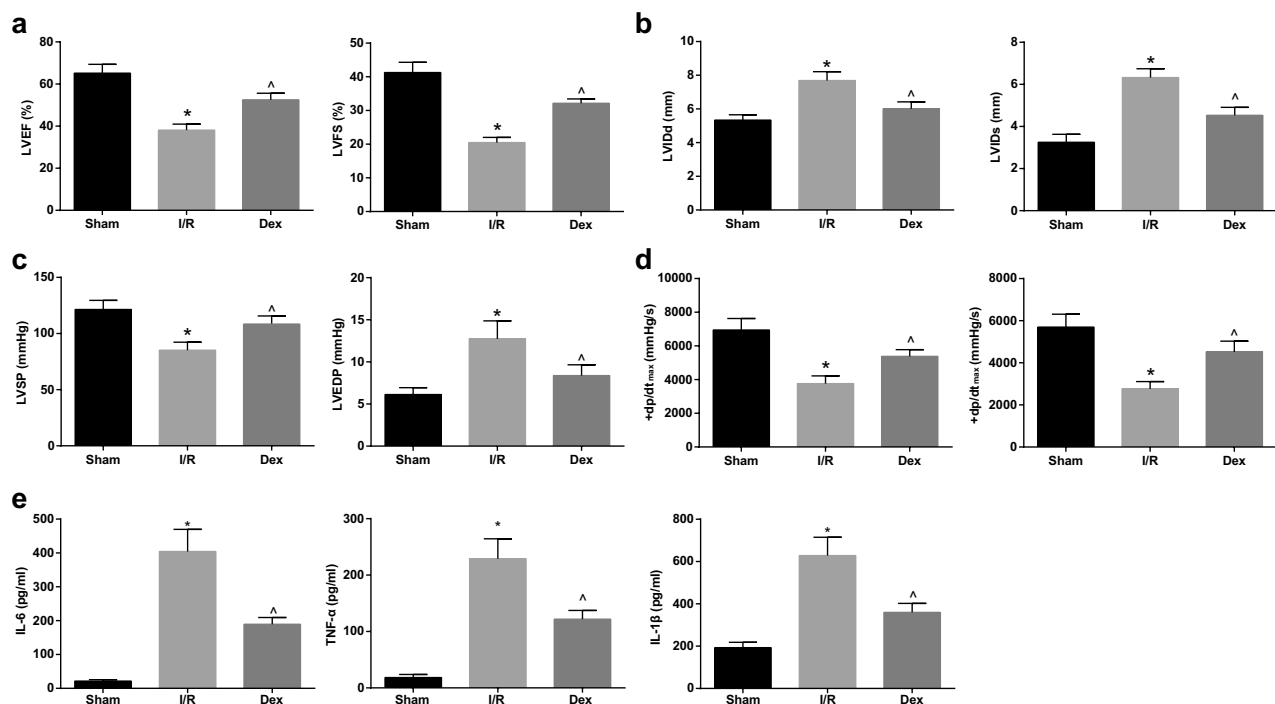


Figure 1. Dex improves cardiac function and reduces inflammatory factor contents in MI/RI mice. (a), Changes of LVEF and LVES in mice after Dex treatment. (b), Changes of LVIDs and LVIDd in mice after Dex treatment. (c), Changes of LVSP and LVEDP in mice after Dex treatment. (d), Changes of \pm dp/dt_{max} in mice after Dex treatment. (e), ELISA tested changes of IL-6, TNF- α and IL-1 β levels in mice after Dex treatment. * *P* < 0.01 vs. the sham group. ^ *P* < 0.01 vs. the I/R group. n = 10. Measurement data were indicated as mean \pm standard deviation. Comparisons among multiple groups were assessed by one-way ANOVA followed by Tukey's post hoc test.

Dex alleviates myocardial damage, decreases collagen fibers and Ltb4r1 expression while increases miR-138-5p expression in myocardial tissues of MI/RI mice

HE staining displayed that (Figure 2(a)) neatly arranged cardiomyocytes, clear cytoplasm texture, obvious nucleus, and intercellular junction were presented in normal mice. In mice with MI/RI, it was seen that myocardial fibers were sparsely arranged, myofilament was broken, cytoplasm was reduced or even deleted, a large number of cell nuclear concentration, fragmentation, and inflammatory cell infiltration appeared, and cell connection was disappeared. Treated with Dex, mice were characterized with slightly disordered cardiomyocytes, decreased cytoplasm, and less inflammatory cells.

Masson staining presented that (Figure 2(b, Figure 2c)) normal mice were displayed with a small amount of collagen fiber precipitation in myocardial stroma while MI/RI mice with a large number of precipitation. Upon treatment with Dex, the collagen fiber precipitation was reduced. CVF increased in mice with MI/RI while they decreased upon treatment with Dex.

Immunohistochemistry demonstrated (Figure 2(d–f)) a small amount of brown Collagen and Collagen III in the stroma and blood vessels of cardiomyocytes in normal mice. However, MI/RI mice showed elevated Collagen and Collagen III. Moreover, when treated with Dex, mice were manifested with decreased Collagen and Collagen III.

RT-qPCR and western blot assay suggested that (Figure 2(g–i)) miR-138-5p reduced and Ltb4r1 elevated in MI/RI mice while they presented the opposite trends if treated with Dex. It was suggested that Dex improved myocardial injury, reduced collagen fibers, up-regulated miR-138-5p and down-regulated Ltb4r1 in myocardial tissues of MI/RI mice.

Restored miR-138-5p ameliorates cardiac function and suppresses inflammatory factor contents in MI/RI mice

It was revealed by cardiac ultrasound detection, hemodynamic detection, and ELISA that (Figure

3(a–e)) miR-138-5p restoration-enhanced levels of LVEF, LVES, LVSP, and $\pm dp/dt_{max}$ while degraded levels of LVIDs, LVIDd, LVEDP, IL-6, TNF- α and IL-1 β . However, miR-138-5p depletion caused the completely opposite trends of these parameters. It was implied that miR-138-5p up-regulation improved the cardiac function and impaired inflammatory reaction while miR-138-5p down-regulation worsened cardiac function and promoted inflammation reaction in MI/RI mice.

Up-regulating miR-138-5p relieves myocardial damage and reduces content of collagen fibers in myocardial tissues of MI/RI mice

It was reported by HE staining that (Figure 4(a)) mice treated with Ad-Ctr and Ad-Neg showed sparse and disordered myocardial fibers, broken myofilament, decreased or depleted cytoplasm, condensed or fragmented nucleus, and infiltrated inflammatory cells. However, in mice treated with Ad-miR-138-5p, slightly disordered cardiomyocytes, decreased cytoplasm, and few infiltrated inflammatory cells were realized. Myocardial injury in mice treated with Ad-miR-138-5p-i was more serious than that in mice treated with Ad-Neg.

Masson staining showed that (Figure 4(b, Figure 4c)) mice treated with Ad-Ctr and Ad-Neg showed a large number of collagen fiber precipitation in myocardial stroma. However, Ad-miR-138-5p treatment suppressed the precipitation while Ad-miR-138-5p-i caused most precipitation of collagen fibers in myocardial stroma. miR-138-5p elevation reduced CVF while miR-138-5p knock-down heightened CVF.

It was presented by immunohistochemistry, RT-qPCR and western blot assay that (Figure 4(d–i)) miR-138-5p up-regulation decreased Collagen I, Collagen III and Ltb4r1 expression, and elevated miR-138-5p expression whereas miR-138-5p degradation worked out the opposite effects on those factors.

Above all, up-regulating miR-138-5p attenuated the myocardial injury and reduced the content of collagen fibers in MI/RI mice, while down-regulation of miR-138-5p aggravated myocardial

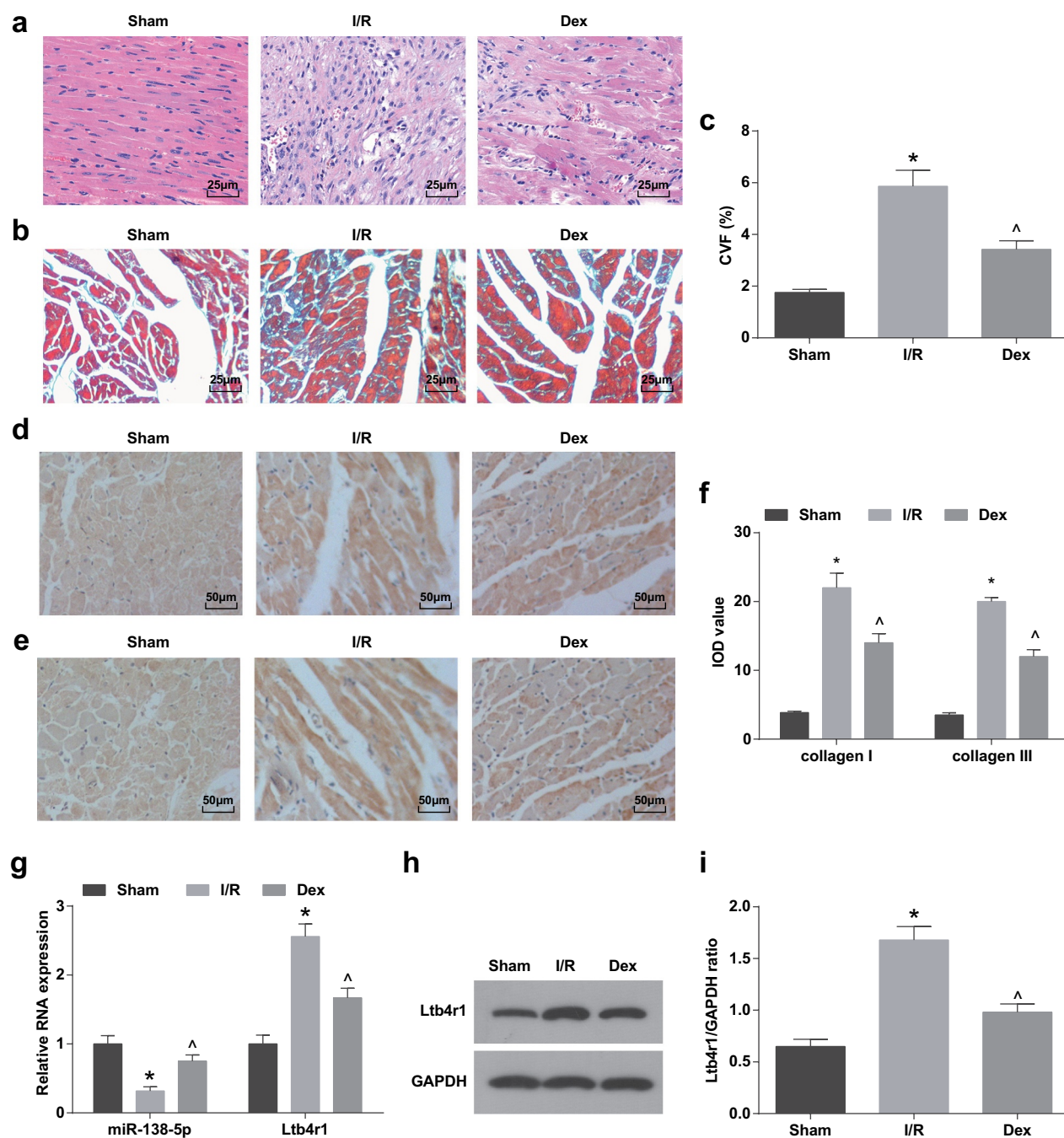


Figure 2. Dex alleviates myocardial damage, decreases content of collagen fibers and Ltb4r1 expression while increases miR-138-5p expression in myocardial tissues of MI/R mice. (a), HE staining tested the pathological changes of cardiomyocytes in mice after Dex treatment. (b), Masson staining tested the collagen fibers precipitation in myocardial stroma after Dex treatment. (c), Changes of CVF content in myocardial stroma after Dex treatment. (d), Immunohistochemistry tested Collagen I expression after Dex treatment. (e), Immunohistochemistry tested Collagen III expression after Dex treatment. (f), The area changes of Collagen I and Collagen III after Dex treatment. (g), RT-qPCR tested miR-138-5p and Ltb4r1 mRNA expression after Dex treatment. (h), Protein bands of Ltb4r1 after Dex treatment. (i), Western blot assay measured the protein expression of Ltb4r1 after Dex treatment. * $P < 0.01$ vs. the sham group. ^ $P < 0.01$ vs. the I/R group. $n = 10$. Measurement data were indicated as mean \pm standard deviation. Comparisons among multiple groups were assessed by one-way ANOVA followed by Tukey's post hoc test.

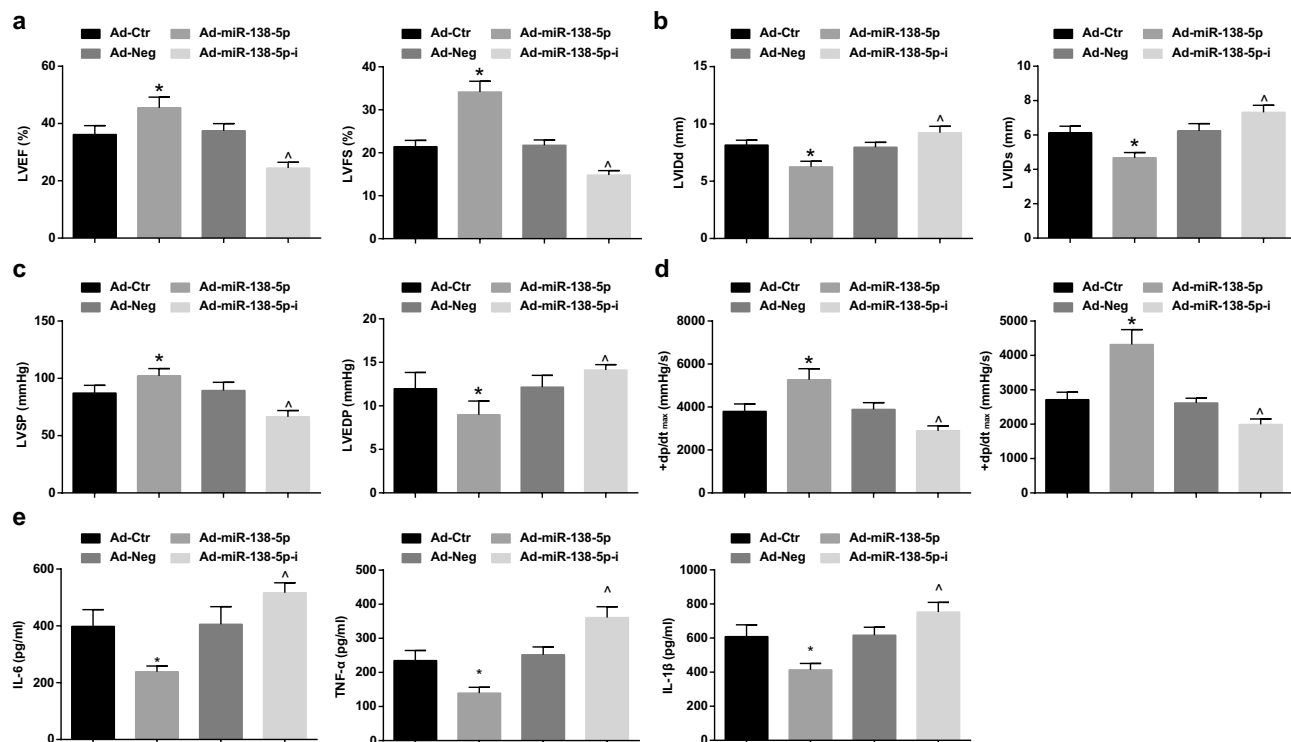


Figure 3. Restored miR-138-5p ameliorates cardiac function and inhibits inflammatory factor contents in MI/RI mice. (a), Changes of LVEF and LVES in mice after regulation of miR-138-5p. (b), Changes of LVIDs and LVIDd in mice after regulation of miR-138-5p. (c), Changes of LVSP and LVEDP in mice after regulation of miR-138-5p. (d), Changes of $\pm dp/dt_{max}$ in mice after regulation of miR-138-5p. (e), ELISA tested changes of IL-6, TNF- α and IL-1 β levels in mice after relation of miR-138-5p. * $P < 0.01$ vs. the Ad-Ctr group. ^ $P < 0.01$ vs. the Ad-Neg group. $n = 10$. Measurement data were indicated as mean \pm standard deviation. Comparisons among multiple groups were assessed by one-way ANOVA followed by Tukey's post hoc test.

injury and increased the content of collagen fibers in MI/RI mice.

Suppression of miR-138-5p reverses the effect of Dex on improved cardiac function and reduced inflammatory factor contents of MI/RI mice

Cardiac ultrasound detection, hemodynamic detection, and ELISA presented that (Figure 5(a-e)): miR-138-5p down-regulation followed by Dex treatment inhibited the levels of LVEF, LVES, LVSP and $\pm dp/dt_{max}$ and raised levels of LVIDs, LVIDd, LVEDP, IL-6, TNF- α , and IL-1 β . Ltb4r1 down-regulation followed by Dex treatment and miR-138-5p depletion-heightened levels of LVEF, LVES, LVSP and $\pm dp/dt_{max}$ while decreased levels of LVIDs, LVIDd, LVEDP, IL-6, TNF- α , and IL-1 β in mice. To conclude, depleting miR-138-5p reversed the effects of Dex on cardiac function and inflammation reaction in mice with MI/RI while knocking down Ltb4r1 also mitigated miR-138-5p depletion-induced effects.

miR-138-5p knockdown reverses the effect of Dex on myocardial damage and collagen fibers content in myocardial tissues of MI/RI mice

It was revealed by HE staining and Masson staining that (Figure 6(a, Figure 6b)) in mice treated with Dex + Ad-Neg, or Dex + Ad-miR-138-5p-i + si-Ltb4r1, cardiomyocytes were slightly disordered, cytoplasm decreased and less inflammatory cells infiltrated, and a small amount of collagen fibers were deposited in myocardial stroma. In mice treated with Dex + miR-138-5p-i, or Dex + Ad-miR-138-5p-i + si-NC, myocardial fibers were sparsely and disorderly arranged, a large number of broken nucleus were concentrated and inflammatory cells were infiltrated with a large number of collagen fibers precipitation in myocardial stroma. MiR-138-5p down-regulation followed by Dex treatment enhanced CVF while Ltb4r1 silencing followed by Dex treatment and miR-138-5p inhibition degraded CVF (Figure 6(c)).

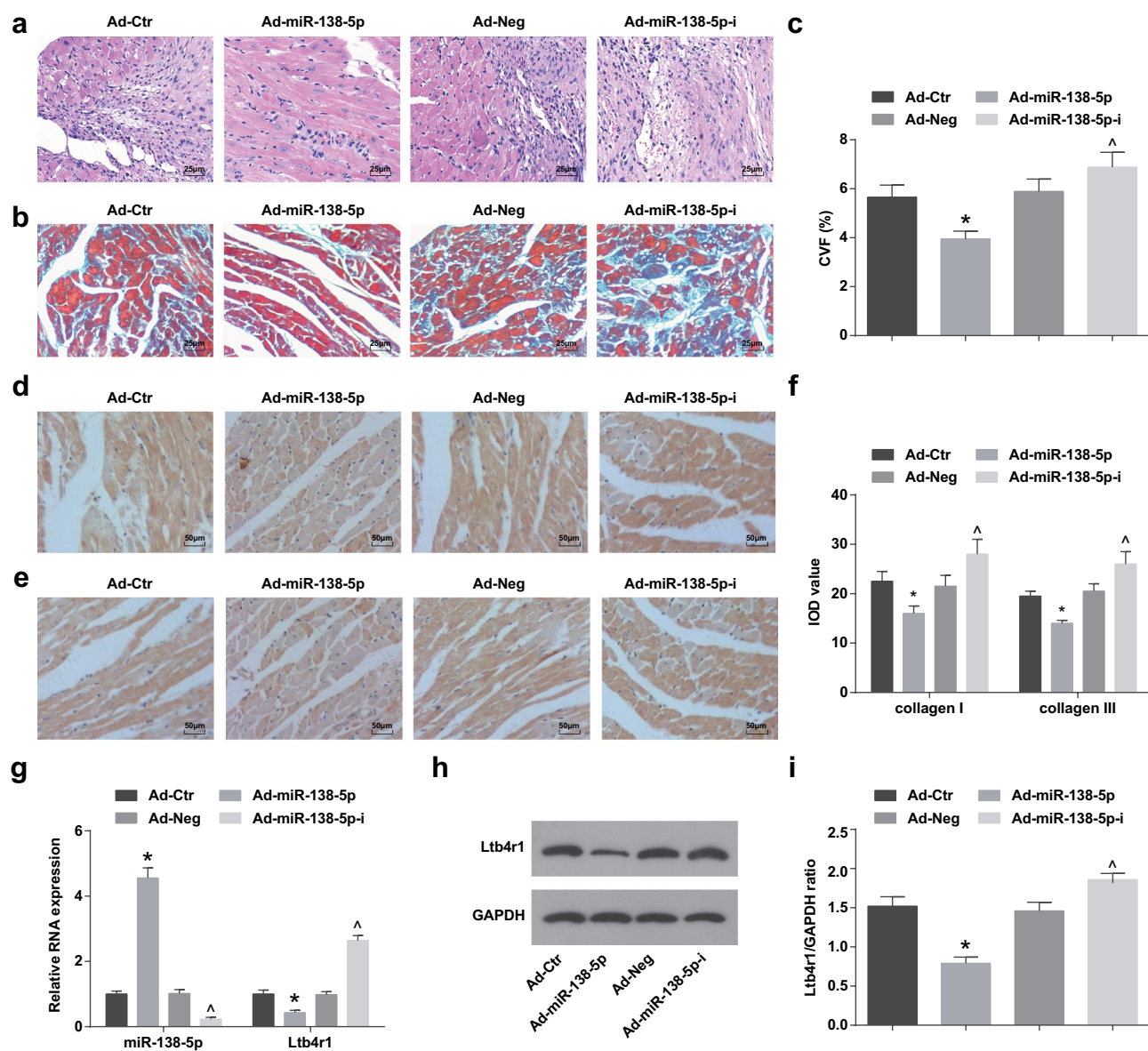


Figure 4. Up-regulating miR-138-5p attenuates myocardial damage and reduces content of collagen fibers in myocardial tissues of MI/RI mice after regulation of miR-138-5p. (a), HE staining tested the pathological changes of cardiomyocytes in mice after regulation of miR-138-5p. (b), Masson staining tested the collagen fibers precipitation in myocardial stroma after regulation of miR-138-5p. (c), Changes of CVF content in myocardial stroma after regulation of miR-138-5p. (d), Immunohistochemistry tested Collagen I expression after regulation of miR-138-5p. (e), Immunohistochemistry tested Collagen III expression after regulation of miR-138-5p. (f), The area changes of Collagen I and Collagen III after regulation of miR-138-5p. (g), RT-qPCR tested miR-138-5p and Ltb4r1 mRNA expression after regulation of miR-138-5p. (h), Protein bands of Ltb4r1 after regulation of miR-138-5p. (i), Western blot assay measured the protein expression of Ltb4r1 after regulation of miR-138-5p. * $P < 0.01$ vs. the Ad-Ctr group. ^ $P < 0.01$ vs. the Ad-Neg group. $n = 10$. Measurement data were indicated as mean \pm standard deviation. Comparisons among multiple groups were assessed by one-way ANOVA followed by Tukey's post hoc test.

It was presented by immunohistochemistry, RT-qPCR, and western blot assay that (Figure 6(d-i)) Ad-miR-138-5p-i reversed the effects of Dex on Collagen I, Collagen III, Ltb4r1 and miR-138-5p expression. Down-regulating Ltb4r1 mitigated miR-138-5p inhibition-induced effects on the same parameters.

It was concluded that miR-138-5p knockdown reversed the effect of Dex on myocardial damage and collagen fibers in MI/RI mice. Down-regulating Ltb4r1 reversed miR-138-5p inhibition-induced effects on myocardial damage and collagen fibers in MI/RI mice.

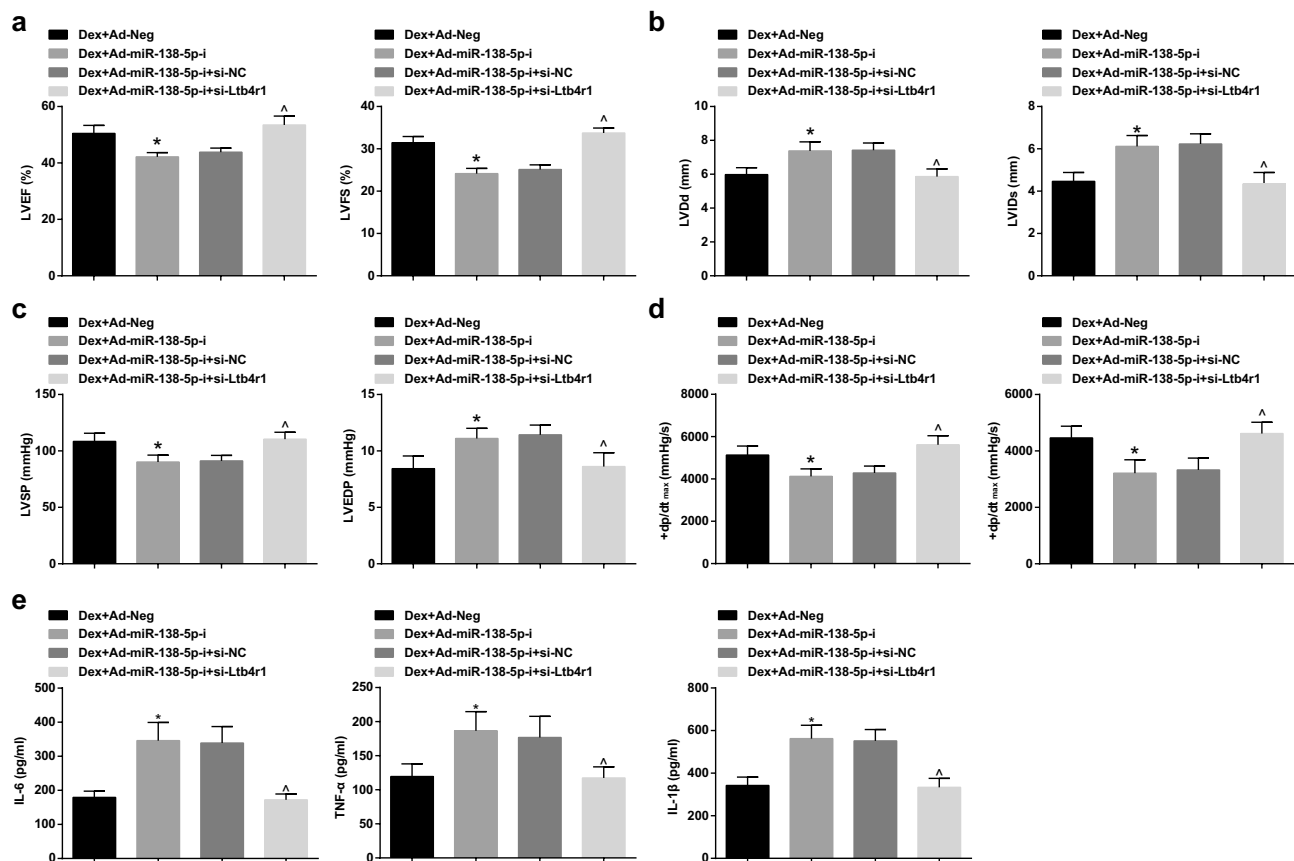


Figure 5. Down-regulation of miR-138-5p reverses the effect of Dex on cardiac function and inflammatory factor levels of MI/RI mice in the rescue experiment. (a), Changes of LVEF and LVES in mice in the rescue experiment. (b), Changes of LVIDs and LVIDd in mice in the rescue experiment. (c), Changes of LVSP and LVEDP in mice in the rescue experiment. (d), Changes of $\pm dp/dt_{max}$ in mice in the rescue experiment. (e), ELISA tested changes of IL-6, TNF- α and IL-1 β levels in mice in the rescue experiment. * $P < 0.01$ vs. the Dex + Ad-Neg group. ^ $P < 0.01$ vs. the Dex + Ad-miR-138-5p-i + si-NC group. $n = 10$. Measurement data were indicated as mean \pm standard deviation. Comparisons among multiple groups were assessed by one-way ANOVA followed by Tukey's post hoc test.

MiR-138-5p directly targets to Ltb4r1

The target relationship between Ltb4r1 and miR-138-5p was predicted by bioinformatics software (Figure 7(a)). Dual luciferase reporter gene assay revealed that (Figure 7(b)) the luciferase activity was decreased in cells with co-transfection of Ltb4r1-WT and miR-138-5p mimic. It was suggested that Ltb4r1 was a target gene of miR-138-5p.

Discussion

MI/RI is an inevitable secondary injury process of ischemic heart disease, and refers to the sudden recovery of blood flow in ischemic myocardium, which aggravates the death of cardiomyocytes and the infarction, and results in the deterioration of cardiac function [21]. A previous study has

presented the effect of Dex preconditioning on the I/R injury in the aged rats [22]. Besides that, overexpression of miR-138 is surveyed to suppress cardiomyocyte apoptosis induced by hypoxia [23]. With reference to an experiment conducted by Bitencourt *et al.*, LTB4 receptor antagonists exert cardioprotective effect on myocardial I/R in mice [24]. Thus, our objective was to investigate the effect of Dex on ventricular remodeling in mice affected by MI/RI by mediating miR-138-5p and Ltb4r1.

At first, it was manifested that miR-138-5p was decreased and Ltb4r1 was elevated in myocardial tissues of MI/RI mice. Recently, a study has pointed out that miR-138 expression trends toward a decrease after MI/RI [11]. Another study has also pictured the reduced miR-138 expression in cardiomyocytes through hypoxia

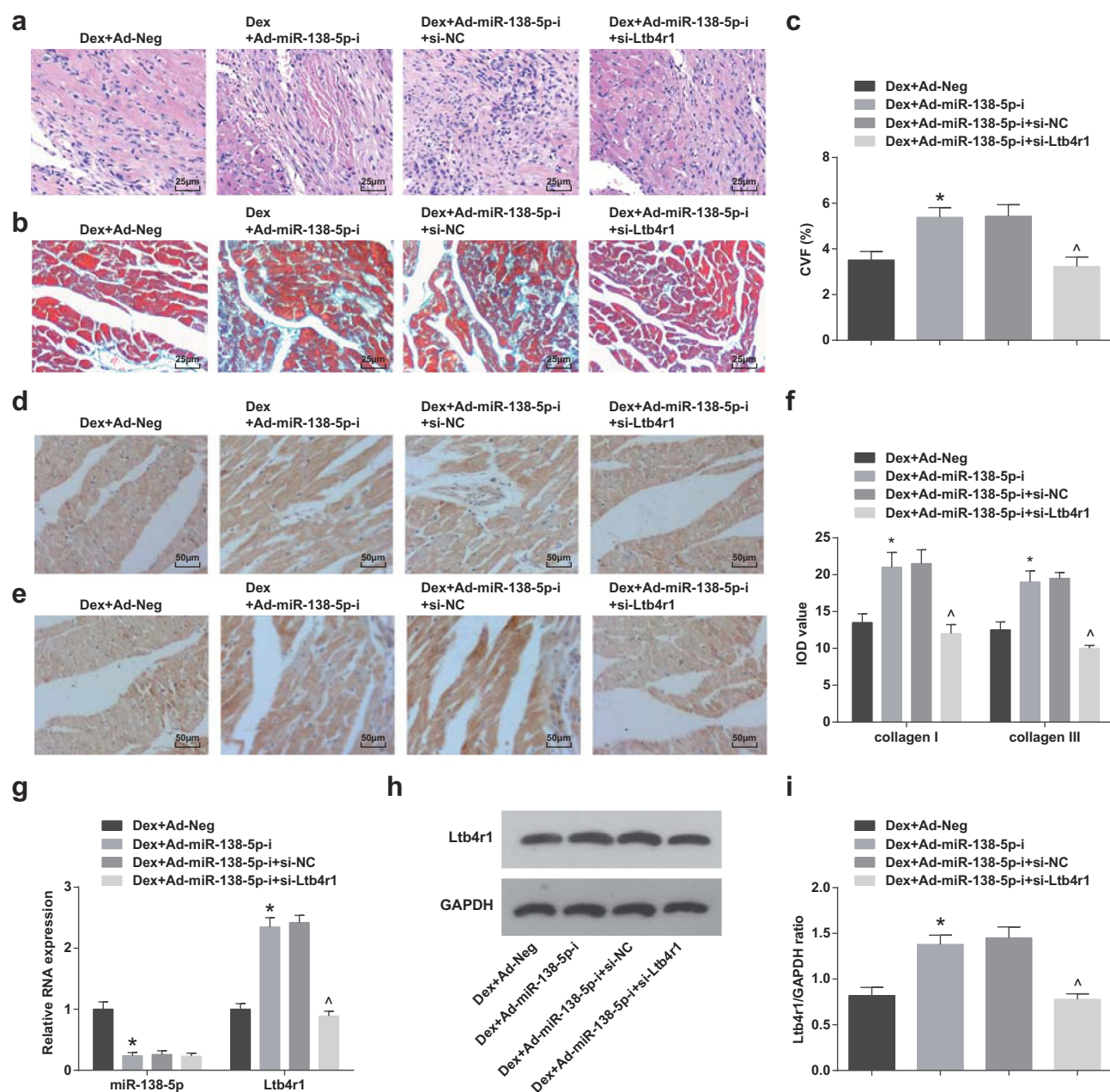


Figure 6. Low expression of miR-138-5p reverses the effect of Dex on myocardial damage and collagen fibers content in myocardial tissues of MI/RI mice. (a), HE staining tested the pathological changes of cardiomyocytes in mice in the rescue experiment. (b), Masson staining tested the collagen fibers precipitation in myocardial stroma in the rescue experiment. (c), Changes of CVF content in myocardial stroma in the rescue experiment. (d), Immunohistochemistry tested Collagen I expression in the rescue experiment. (e), Immunohistochemistry tested Collagen III expression in the rescue experiment. (f), The area changes of Collagen I and Collagen III in the rescue experiment. (g), RT-qPCR tested miR-138-5p and Ltb4r1 mRNA expression in the rescue experiment. (h), Protein bands of Ltb4r1 in the rescue experiment. (i), Western blot assay measured the protein expression of Ltb4r1 in the rescue experiment. * $P < 0.01$ vs. the Dex + Ad-Neg group. ^ $P < 0.01$ vs. the Dex + Ad-miR-138-5p-i + si-NC group. $n = 10$. Measurement data were indicated as mean \pm standard deviation. Comparisons among multiple groups were assessed by one-way ANOVA followed by Tukey's post hoc test.

treatment [25]. It is reported that LTB expression in serum, synovial fluid, and synovial tissues is up-regulated in rheumatoid arthritis (RA) patients, indicating that LTB and BLT1 likely are involved in the pathogenesis of human RA [26].

Furthermore, it is disclosed that BLT1 expression is dramatically heightened after subarachnoid hemorrhage [27]. Our study reported that miR-138-5p directly targeted to Ltb4r1. However, there is no research yet to prove the target

especially focusing on further biomarkers related to miR-138 activity.

From these results, it is clear that Dex could ameliorate ventricular remodeling of MI/RI mice by up-regulating miR-138-3p and down-regulating Ltb4r1. Thus, Dex and miR-138-3p/Ltb4r1 may serve as a potential target for the ventricular remodeling of MI/RI. Owing to the limitation of known researches, the effects of miR-138-3p and Ltb4r1 on MI/RI need to be monitored rigorously and presented appropriately in the future clinical trials.

Acknowledgments

We would like to acknowledge the reviewers for their helpful comments on this paper.

Disclosure statement

The authors declare that they have no conflicts of interest.

References

- [1] Panagiotou A, Trendelenburg M, Osthoff M. The lectin pathway of complement in myocardial ischemia/reperfusion injury-review of its significance and the potential impact of therapeutic interference by C1 esterase inhibitor. *Front Immunol.* 2018;9:1151.
- [2] Huang ZQ, Xu W, Wu J-L, et al. MicroRNA-374a protects against myocardial ischemia-reperfusion injury in mice by targeting the MAPK6 pathway. *Life Sci.* 2019;232:116619.
- [3] Xie B, Liu, X, Yang, J, et al. PIAS1 protects against myocardial ischemia-reperfusion injury by stimulating PPARgamma SUMOylation. *BMC Cell Biol.* 2018;19(1):24.
- [4] Wang L, Ma H, Xue Y, et al. Berberine inhibits the ischemia-reperfusion injury induced inflammatory response and apoptosis of myocardial cells through the phosphoinositide 3-kinase/RAC-alpha serine/threonine-protein kinase and nuclear factor-kappaB signaling pathways. *Exp Ther Med.* 2018;15(2):1225–1232.
- [5] Song C-L, Liu B, Diao H-Y, et al. The protective effect of MicroRNA-320 on left ventricular remodeling after myocardial ischemia-reperfusion injury in the rat model. *Int J Mol Sci.* 2014;15(10):17442–17456.
- [6] Kundra TS, Thimmarayappa A, Dhananjaya M, et al. Dexmedetomidine for prevention of skeletal muscle ischaemia-reperfusion injury in patients with chronic limb ischaemia undergoing aortobifemoral bypass surgery: A prospective double-blind randomized controlled study. *Ann Card Anaesth.* 2018;21(1):22–25.
- [7] Xu Z, Wang D, Zhou Z, et al. Dexmedetomidine attenuates renal and myocardial ischemia/reperfusion injury in a dose-dependent manner by inhibiting inflammatory response. *Ann Clin Lab Sci.* 2019;49(1):31–35.
- [8] He Z, Ruan X, Liu X, et al. FUS/circ_002136/miR-138-5p/SOX13 feedback loop regulates angiogenesis in Glioma. *J Exp Clin Cancer Res.* 2019;38(1):65.
- [9] Donato L, Bramanti P, Scimone C, et al. miRNA expression profile of retinal pigment epithelial cells under oxidative stress conditions. *FEBS Open Bio.* 2018;8(2):219–233.
- [10] Bai X, Shao J, Zhou S, et al. Inhibition of lung cancer growth and metastasis by DHA and its metabolite, RvD1, through miR-138-5p/FOXO1 pathway. *J Exp Clin Cancer Res.* 2019;38(1):479.
- [11] Liu Y, Zou J, Liu X, et al. MicroRNA-138 attenuates myocardial ischemia reperfusion injury through inhibiting mitochondria-mediated apoptosis by targeting HIF1-alpha. *Exp Ther Med.* 2019;18(5):3325–3332.
- [12] Zhu H, Xue H, Jin QH, Xue H, Jin QH, et al. MiR-138 protects cardiac cells against hypoxia through modulation of glucose metabolism by targeting pyruvate dehydrogenase kinase 1. *Biosci Rep.* 2017;37(6). doi:10.1042/BSR20170296.
- [13] Ying W, Wollam J, Ofrecio JM, et al. Adipose tissue B2 cells promote insulin resistance through leukotriene LTB4/LTB4R1 signaling. *J Clin Invest.* 2017;127(3):1019–1030.
- [14] Hansen AK, Indrevik J-T, Figenschau Y, et al. Human articular chondrocytes express functional leukotriene B4 receptors. *J Anat.* 2015;226(3):268–277.
- [15] Zhang L, Huang J, Dong R, et al. Therapeutic potential of BLT1 antagonist for COPD: involvement of inducing autophagy and ameliorating inflammation. *Drug Des Devel Ther.* 2019;13:3105–3116.
- [16] Sun M, Wang R, Han Q. Inhibition of leukotriene B4 receptor 1 attenuates lipopolysaccharide-induced cardiac dysfunction: role of AMPK-regulated mitochondrial function. *Sci Rep.* 2017;7:44352.
- [17] de Hoog VC, Bovens SM, de Jager SCA, et al. BLT1 antagonist LSN2792613 reduces infarct size in a mouse model of myocardial ischaemia-reperfusion injury. *Cardiovasc Res.* 2015;108(3):367–376.
- [18] Ferdinandy P, Schulz R, Baxter GF. Interaction of cardiovascular risk factors with myocardial ischemia/reperfusion injury, preconditioning, and postconditioning. *Pharmacol Rev.* 2007;59(4):418–458.
- [19] Zhang JJ, Peng K, Zhang J, et al. Dexmedetomidine preconditioning may attenuate myocardial ischemia/reperfusion injury by down-regulating the HMGB1-TLR4-MyD88-NF-small ka, CyrillicB signaling pathway. *PLoS One.* 2017;12(2):e0172006.

- [20] Yang Y, Yang J, Liu X-W, et al. Down-regulation of miR-327 alleviates ischemia/reperfusion-induced myocardial damage by targeting RP105. *Cell Physiol Biochem*. 2018;49(3):1049–1063.
- [21] Liu Q, Li Z, Liu Y, et al. Hydromorphone postconditioning protects isolated rat heart against ischemia-reperfusion injury via activating P13K/Akt/eNOS signaling. *Cardiovasc Ther*. 2018;36(6):e12481.
- [22] Dong J, Guo X, Yang S, et al. The effects of dexmedetomidine preconditioning on aged rat heart of ischemia reperfusion injury. *Res Vet Sci*. 2017;114:489–492.
- [23] Xiong H, Luo T, He W, et al. Up-regulation of miR-138 inhibits hypoxia-induced cardiomyocyte apoptosis via down-regulating lipocalin-2 expression. *Exp Biol Med (Maywood)*. 2016;241(1):25–30.
- [24] Bitencourt CS, Bessi VL, Huynh DN, et al. Cooperative role of endogenous leucotrienes and platelet-activating factor in ischaemia-reperfusion-mediated tissue injury. *J Cell Mol Med*. 2013;17(12):1554–1565.
- [25] Zhang X, Qin Q, Dai H, et al. Emodin protects H9c2 cells from hypoxia-induced injury by up-regulating miR-138 expression. *Braz J Med Biol Res*. 2019;52(3):e7994.
- [26] Miyabe Y, Miyabe C, Luster AD. LTB4 and BLT1 in inflammatory arthritis. *Semin Immunol*. 2017;33:52–57.
- [27] Ye ZN, Zhuang Z, Wu L-Y, et al. Expression and cell distribution of leukotriene B4 receptor 1 in the rat brain cortex after experimental subarachnoid hemorrhage. *Brain Res*. 2016;1652:127–134.
- [28] He L, Hao S, Wang Y, et al. Dexmedetomidine preconditioning attenuates ischemia/reperfusion injury in isolated rat hearts with endothelial dysfunction. *Biomed Pharmacother*. 2019;114:108837.
- [29] Zhang J, Zhang -J-J, Peng K, et al. Dexmedetomidine-induced cardioprotection is mediated by inhibition of high mobility group box-1 and the cholinergic anti-inflammatory pathway in myocardial ischemia-reperfusion injury. *PLoS One*. 2019;14(7):e0218726.
- [30] Zhang J, Jiang H, Liu DH, et al. Effects of dexmedetomidine on myocardial ischemia-reperfusion injury through PI3K-Akt-mTOR signaling pathway. *Eur Rev Med Pharmacol Sci*. 2019;23(15):6736–6743.
- [31] Li JB, Wang HY, Yao Y, et al. Overexpression of microRNA-138 alleviates human coronary artery endothelial cell injury and inflammatory response by inhibiting the PI3K/Akt/eNOS pathway. *J Cell Mol Med*. 2017;21(8):1482–1491.
- [32] Saito Y, Watanabe K, Fujioka D, et al. Disruption of group IVA cytosolic phospholipase A2 attenuates myocardial ischemia-reperfusion injury partly through inhibition of TNF- α -mediated pathway. *Am J Physiol Heart Circ Physiol*. 2012;302(10):H2018–30.
- [33] Donato L, Scimone C, Alibrandi S, et al. Transcriptome analyses of lncRNAs in A2E-stressed retinal epithelial cells unveil advanced links between metabolic impairments related to oxidative stress and retinitis pigmentosa. *Antioxidants (Basel)*. 2020;9(4). doi:10.3390/antiox9040318.
- [34] Donato L, D'Angelo R, Alibrandi S, et al. Effects of A2E-induced oxidative stress on retinal epithelial cells: new insights on differential gene response and retinal dystrophies. *Antioxidants (Basel)*. 2020;9(4). doi:10.3390/antiox9040307.
- [35] Donato L, Scimone C, Alibrandi S, et al. Discovery of GLO1 new related genes and pathways by RNA-Seq on A2E-stressed retinal epithelial cells could improve knowledge on retinitis pigmentosa. *Antioxidants (Basel)*. 2020;9(5).doi:10.3390/antiox9050416.
- [36] Jeong C, Ma J, Lai W. RALBP1 regulates oral cancer cells via Akt and is a novel target of miR-148a-3p and miR-148b-3p. *J Oral Pathol Med*. 2019;48(10):919–928.
- [37] Scimone C, Donato L, Esposito T, et al. A novel RLBPI gene geographical area-related mutation present in a young patient with retinitis punctata albescens. *Hum Genomics*. 2017;11(1):18.
- [38] Rinaldi C, Bramanti P, Scimone C, et al. Relevance of CCM gene polymorphisms for clinical management of sporadic cerebral cavernous malformations. *J Neurol Sci*. 2017;380:31–37.